Detecting pediatric foot deformities using plantar pressure measurements: A semi-supervised approach

Detecting pediatric foot deformities using plantar pressure measurements: A semi-supervised approach

K Ramakrishna Kini, Muddu Madakyaru, Fouzi Harrou (Senior Member, IEEE), Ying Sun

***Abstract*—This paper presents a semi-supervised data-driven approach to identify pediatric foot deformities using foot plantar pressure measurements. Essentially, the developed approach merges the desirable features of the kernel principal components analysis as a feature extractor and the Kantorovich Distance-driven monitoring scheme for detecting pediatric foot deformities. For extending the flexibility of the proposed scheme, kernel density estimation based nonparametric decision threshold is adopted. The method is assessed via publically available data containing three types of footsteps (i.e., normal, flat, and cavus). The detection results show that the method proved promising results, thus, outperforming commonly applied monitoring schemes.**

***Index Terms*—Foot deformities, plantar pressure sensors, anomaly detection, unlabeled data, kernel PCA, Kantorovich Distance.**

I. Introduction

Measurements of plantar pressure are usually employed in clinical to assess the walking function of a human foot and identify some diseases, like diabetes [1]. Several studies showed the importance of these measurements for identifying foot pathology [2]. For instance, the study in [3] studied plantar pressure during the gait to investigate foot deformity and foot loading in diabetic neuropathy. Of course, information extracted from plantar pressure measurements is an important element to aid in determining the impairments related to different musculoskeletal and neurological disorders.

Monitoring natural pathologies of the foot are undoubtedly necessary for avoiding pain in physical activities or any abnormalities in the mechanics of natural movements. Accordingly, designing efficient footprint detection criteria and monitoring systems is crucial for enabling children to correctly develop a functional locomotor system [1]. There are two pathological symptoms: flat foot and arched foot. The flat foot is characterized by the arches on the inside of the feet that are flattened. This permits the entire soles of the feet to touch the floor when standing up. Flatfeet could occur due to inappropriate development of the arches during childhood or after an injury, or from the simple wear-and-tear stresses of age. While flatfeet may result in problems in the ankles and knees because the alignment of the legs could be altered, an arched foot may result in stiffening of the toes. Different factors could increase the risk of foot deformities, including obesity, diabetes, and aging. Thus, accurately detecting pediatric foot deformities provides information for early diagnosis and physical rehabilitation.

Over recent years, there is increased interest in developing sensitive detectors for the early identification of pediatric foot deformities. For instance, in [4], a supervised approach using a support vector machine (SVM) is applied for plantar-pressure-based ambulatory classification based on low-cost smart shoes. Results showed that SVM reached recognition rates up to 95.2% in discriminating between the three ambulatory activities. Recently, the study in [5] proposed an embedded system to discriminate the type of footprint (i.e., normal, flat, and arched) of preschool and school children. To this end, several supervised machine learning classifiers, including k-nearest neighbors (k-NN), Naive Bayes, and decision tree classifiers, were applied to identify the type of footprint based on data collected from the resistive pressure sensors in the foot. Results revealed the superior classification performance of the k-NN algorithm. However, most existing approaches for foot deformities detection are based on shallow supervised methods that need labeled data in training. However, obtaining labeled data is not obvious, and can consume much time, requiring huge human efforts and knowledge inputs [6]. Therefore, this work aims to develop a semi-supervised data-driven approach for foot deformities detection based on unlabeled data.

This paper presents a data-driven approach to identify pediatric foot deformities using resistive pressure sensors distributed in three areas: forefoot, midfoot and rearfoot. A multivariate scheme based on Kernel PCA (KPCA) is integrated with Kantorovich Distance (KD) to efficiently identify foot deformities. Unlike PCA employing linear PCA, KPCA can extract non-linear features from multivariate data. The KD-driven scheme is applied to the residuals from the KPCA modeling framework. The KD metric involves a one-to-one comparison between the segments of two distributions, enabling it to capture the critical details in the data. The kernel density estimation (KDE) approach is used to compute the detection threshold for the KD-based approach in this study. Unlike supervised algorithms, the KPCA-KD approach, as a semi-supervised approach, only employs the plantar pressure data of normal feet to train the detection model, making them more attractive for detecting foot deformities since it

K.R. Kini is with the Department of Instrumentation and Control Engineering, Manipal Institute of Technology, Manipal Academy of Higher Education, Manipal 576104, India

M. Madakyaru is with the Department of Chemical Engineering, Manipal Institute of Technology, Manipal Academy of Higher Education, Manipal 576104, India

F. Harrou and Y. Sun are with the Computer, Electrical and Mathematical Sciences and Engineering Division, King Abdullah University of Science and Technology, Thuwal 23955-6900, Saudi Arabia

Corresponding Author: Fouzi Harrou (email: fouzi.harrou@kaust.edu.sa)

This work was supported by the King Abdullah University of Science and Technology, Office of Sponsored Research (OSR) under Award OSR-2019-CRG7-3800

is not always easy to get accurately labeled data. Publically available data is utilized to assess the proposed approach's detection capacity. The data set contains data about three types of footsteps in children between 11 and 12 years old (i.e., normal, flat, and cavus). For comparison purposes, we applied the PCA, Independent Component Analysis (ICA), and KPCA-based T^2 and squared prediction error (SPE) statistical indicators to identify foot deformities.

The remainder of this paper is organized as follows. The following section briefly describes the preliminary materials like linear PCA, KPCA, and the KD anomaly detector. Then, the KPCA-driven KD anomaly detection technique is discussed. After that, we assess the performance of the proposed approach using a publicly available dataset. Finally, we offer conclusions to this study.

II. Methodology:

A. Principal Component Analysis

PCA is a multivariate technique that transforms data from a higher space to a smaller subspace by retaining data from the original space. Consider a data $\mathbf{X} \in R^{n\times d}$ where covariance matrix is decomposed to have the following [7]:

$$\mathbf{\Sigma} = \frac{\mathbf{X^T X}}{n-1} = \mathbf{P}\Lambda\mathbf{P}^T \tag{1}$$

where $\mathbf{T}$, $\mathbf{P}$ and Λ=diag$(\lambda_1, \lambda_2, \ldots \lambda_m)$ represent score, loading and diagonal matrices that contains eigenvalues of $\mathbf{\Sigma}$. Once useful principal components (PCs) are determined, the PCA model can be represented as a combination of approximated as well as residual matrices:

$$\mathbf{X} = \hat{\mathbf{T}}\hat{\mathbf{P}}^{\mathbf{T}} + \tilde{\mathbf{T}}\tilde{\mathbf{P}}^{\mathbf{T}} \tag{2}$$

Both matrices can reveal useful information about the process, which are evaluated by two statistical indicators which can be defined in the following manner [7]:

$$T^2 = \mathbf{X_{new}}^T\hat{\mathbf{P}}\hat{\mathbf{\Lambda}}^{-1}\hat{\mathbf{P}}^T\mathbf{X_{new}} \tag{3}$$

$$SPE = \mathbf{X_{new}}^T(\mathbf{I} - \hat{\mathbf{P}}\hat{\mathbf{P}}^{\mathbf{T}})\mathbf{X_{new}} \tag{4}$$

An abnormal event is observed whenever the value of statistical metrics crosses the reference threshold.

B. Kernel Principal Component Analysis

The Kernel PCA uses kernel tricks to effectively extract the non-linear details present in the data. For available data, $\mathbf{Z} \in R^{n\times d}$ mapping in feature space is carried out in the following manner [8]:

$$\phi : \Re^m \rightarrow \mathbf{F}^m \tag{5}$$

The computation of co-variance matrix $\mathbf{C}$ is carried out in feature space in the following manner:

$$\mathbf{C} = \frac{1}{n}\sum_{i=1}^{n}\phi(\mathbf{z_i})\phi(\mathbf{z_i})^T, \tag{6}$$

where $\phi(.)$ defines a mapping function. In (6), non-zero eigenvalues of $\mathbf{C}$ are non-negative. Next, the eigenvalue problem $\lambda\mathbf{v} = \mathbf{C^F v}$ is solved to compute the principal components (PCs):

$$\lambda\mathbf{v} = \left(\frac{1}{n}\sum_{j=1}^{n}\phi(\mathbf{z_j})\phi(\mathbf{z_j})^T\right)\mathbf{v} = \frac{1}{n}\sum_{j=1}^{n}\langle\phi(\mathbf{z_j}), \mathbf{v}\rangle\,\phi(\mathbf{z_j}) \tag{7}$$

At each observations, coefficients a_i (i = 1, 2, ... n) are such that:

$$\mathbf{v} = \sum_{i=1}^{n} a_i\phi(\mathbf{z_i}). \tag{8}$$

By the introduction of the kernel matrix $\mathbf{K}$, we have:

$$\lambda\alpha = \frac{1}{n}\mathbf{K}\alpha, \tag{9}$$

where $\alpha = [a_1, a_2, \ldots a_d]^T$. Next, the computation of Kernel PCs takes place using the following expression:

$$t_k = \langle\mathbf{v}_k, \mathbf{\Psi}(\mathbf{z})\rangle = \sum_{j=1}^{n}\alpha_j^k\langle\phi(\mathbf{z_j})\phi(\mathbf{z})\rangle \tag{10}$$

In the equation (9) λ denotes eigenvalues and $\alpha = [a_1, a_2, \ldots a_d]^T$ denotes eigenvectors. Once the reference KPCA model is available, it can detect abnormal events using T^2 and SPE indicators. The T^2 indicator captures variations within the developed KPCA model and can be computed as [9]:

$$T^2 = [t_1, t_2, \ldots, t_p]\Lambda^{-1}[t_1, t_2, \ldots, t_p]^T, \tag{11}$$

where Λ = diag$(\lambda_1 > \lambda_2 > \ldots \lambda_p)$ is a diagonal matrix of eigen values. The variations in the non-model subspace of the model are captured by the SPE indicator represented as:

$$SPE = ||\phi(\mathbf{z}) - \phi(\mathbf{p}(\mathbf{z}))||^2 \tag{12}$$

Abnormal events are identified when both the KPCA-based detection metrics exceed the reference threshold [8].

C. Kantorovich Distance

Kantorovich Distance (KD) is a statistic used to quantify the similarity between two distributions. The fundamental concept of this metric is that the information can be relocated from one distribution to the other based on the theory of optimal mass transport. Notably, the KD statistic relies on a cost function for transporting data between two distributions. The cost function is less for two distributions that are similar and large for two dissimilar distributions. Since abnormal event detection problems make decisions based on comparing normal and potential anomaly data, KD statistic fits well for such situations. The transport theory cost function *l* is defined based on the norm:

$$c(a, b) = ||a - b||^r. \tag{13}$$

The optimal mass transport for cost function *r* in the case *r*=1 is represented as [10]:

$$W_r(A, B) = \left(\inf_{\gamma\in\Gamma(A,B)}\int||a - b||^r d\gamma(a, b)\right)^{1/r}, \tag{14}$$

where $\Gamma(A, B)$ indicates distributions that are joint, and minimum optimal coupling is denoted by γ [10]. When cost function *r*=2, the mass transport function is denoted as Kantorovich

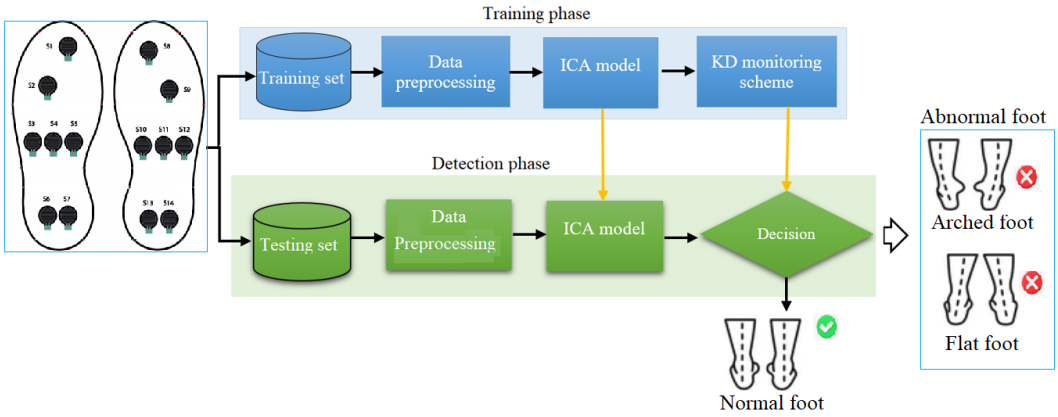

Fig. 1. Flowchart of the detection strategy.

Distance (KD) metric. The KD metric is computed using a step-by-step segmentation process for any two probability distribution functions, A and B. The KD metric is calculated between each segment in distribution A with each segment in distribution B. This ensures all crucial features in the data are captured and, eventually, enhances detection performance [10]. The KPCA model is integrated with the KD metric to yield the KPCA-KD scheme in this work.

D. The proposed KPCA-KD strategy

The main aim of this work is to have a data-driven scheme that can efficiently detect flat and arched deformities based on unlabeled data. A scheme that integrates KPCA modeling with KD-based statistical indicators is proposed in this regard. Figure 1 presents the methodology for determining abnormal deformity. It is worthwhile to notice that the residuals from a data-driven model contain pertinent information, and evaluating them appropriately aids in determining deformities. Broadly speaking, the residuals are around zero in the absence of foot deformities. However, in the case of foot deformities, the residuals deviate significantly from zero. The KPCA model residuals are generated as follows:

$$\mathbf{E} = \phi(\mathbf{Z}) - \phi(\mathbf{Z})\mathbf{v}_p\mathbf{v}_p^T, \tag{15}$$

where $\mathbf{v}_p$ denotes the eigenvectors for dominant PCs.

The proposed KPCA-KD scheme is briefed as follows:

- **Step 1:** Once normal data is available, perform standardization.
- **Step 2:** Develop the reference KPCA model from standardized data.
- **Step 3:** From the model, compute residuals *RS1* as given in equation(15).
- **Step 4:** Compute the threshold for KD-based abnormal event detector using the KDE approach.
- **Step 5:** When new data (possibly having an abnormality) is available, perform standardization.
- **Step 6:** From the model, generate residuals *RS2* for the new data.
- **Step 7:** Compute KD metric between *RS1* and *RS2* using the segmentation process.
- **Step 8:** Declare an abnormal event when the KD metric exceeds the reference threshold.

Note that the decision threshold of conventional monitoring charts is derived based on the Gaussian distribution of the data. However, often in practice, the underlying distribution of data deviates from Gaussianity or is unknown. In such cases, the monitoring results would be unsuitable. Here, a non-parametric KDE method is used to set a detection threshold of the KD-based detector, which extends the flexibility of the proposed approach. First, we use KDE to estimate the distribution of the KD statistic based on anomaly-free data. Given the KD statistic w, the probability distribution function (PDF) through the KDE is computed as follows:

$$\hat{f}(\mathbf{w}) = \frac{1}{nh}\sum_{i=1}^{n} K\left(\frac{\mathbf{w} - \mathbf{w}_i}{h}\right), \tag{16}$$

where $K(.)$ is the kernel function, h is the kernel bandwidth parameter, and n refers to the number of samples. It is worth pointing out that the Gaussian kernel function is commonly utilized.

$$K(\mathbf{w}) = \frac{1}{\sqrt{2\pi}}\exp\left(-\frac{\mathbf{w}^2}{2}\right). \tag{17}$$

Now, the threshold for KD-metric is derived as the $(1-\alpha)$-th quantile of the estimated distribution of the KD statistic, computed via the KDE.

This study uses four statistical scores for quantifying the performance of the studied methods that involves a 2×2 confusion matrix: Precision, Recall, F1-score, and Area under curve (AUC) [11]. For a binary detection problem, the number of true positives (TP), false positives (FP), false negatives (FN), and true negatives (TN) are used to compute these metrics.

$$\text{Recall} = \frac{\text{TP}}{\text{TP} + \text{FN}}. \tag{18}$$

$$\text{Precision} = \frac{\text{TP}}{\text{TP} + \text{FP}}. \tag{19}$$

$$\text{F1} - \text{score} = 2\frac{\text{Precision.Recall}}{\text{Precision} + \text{Recall}} = \frac{2\text{TP}}{2\text{TP} + \text{FP} + \text{FN}}. \tag{20}$$

III. Results and Discussion

The section provides the deformity identification capability of the data-driven scheme based on KPCA-KD. Five scores are utilized to verify the investigated methods' detection capability: anomaly detection rate (ADR), false alarm rate (FAR), Precision, Recall, and F1-Score.

A. Data Description

The experiments are accomplished through actual data from a publicly available database provided in [12], [5]. Fourteen pressure sensors are used to gather pressure data from each foot. Figure 2 illustrates the distribution of the sensors on the right and left foot. For each foot, there are two sensors in the forefoot, three in the midfoot, and three in the heels.

Fig. 2. Distribution pressure sensors in the foots.

The dataset in [12] comprises data with three types of footsteps (i.e., normal, flat, and cavus) in children between 11 and 12 years old. The dataset is relatively small, with 400 data points from the 14 sensors. Specifically, there are 133 data points collected for normal footsteps, 133 for flat footsteps, and 134 for cavus footsteps. For more details on this data, see [12], [5]. In [5], the data are collected using foot biomechanic systems (FBSs).

Table I summarizes the descriptive statistics of each pressure variable from normal feet, which confirm the non-Gaussian distribution of data. It would be challenging for traditional monitoring charts to be constructed based on the Gaussian assumption of data. Accordingly, developing advanced monitoring charts based on KPCA and KD with a nonparametric detection threshold is essential.

B. Detection Results

Initially, the reference PCA, ICA, and KPCA models are developed from the normal footstep data, and eight optimum components are retained in each case. Once the reference models are developed, the next task involves the computation of residuals, and then abnormalities will be identified in the testing footstep data using the KPCA-KD-based scheme.

Sensors	std	Q1	Median	Q3	Skewness	Kurtosis
S1	65.01	944	945	1023	-2.93	16.53
S2	39.65	943	943.5	1023	0.43	1.23
S3	227.14	738.5	949.5	1023	-1.57	4.93
S4	227.14	738.5	949.5	1023	-1.57	4.93
S6	41.93	936	937	1023	0.52	1.33
S7	42.78	936	937	1023	0.43	1.23
S8	109.08	963.5	971	1023	-2.64	9.46
S9	38.75	966	968	1023	-1.79	9.91
S11	227.14	738.5	949.5	1023	-1.57	4.93
S12	385.23	197	534.5	1023	-0.07	1.55
S13	15.91	991	992	1023	0.38	1.24
S14	126.86	956	958	1023	-2.98	10.99

TABLE I
Statistical summary of the normal time-series dataset.

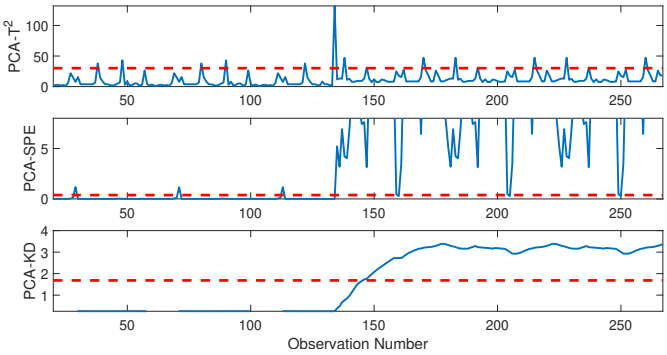

Fig. 3. PCA-driven detection results for cavus deformity: PCA-T^2 (Top) , PCA-SPE (Middle), and PCA-KD (Bottom).

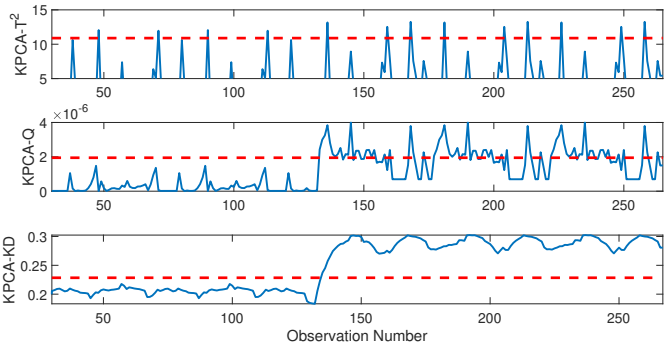

Fig. 4. KPCA-driven detection results for cavus deformity: KPCA-T^2 (Top), KPCA-SPE (Middle), and KPCA-KD (Bottom).

a) Case 1:: In the first experiment, the proposed scheme is assessed in the presence of arched foot deformities. The results of different indicators in identifying this deformity are presented in Table II. From Table II, it may be observed that PCA-SPE and PCA-KD fail in detecting this abnormal situation while the PCA-T^2, KPCA-T^2, KPCA-SPE and KPCA-KD-based schemes can identify easily.The conventional indicators of ICA are unable to precisely identify the abnormality, but the ICA-KD scheme shows fairly better detection. Essentially, the proposed KPCA-KD scheme demonstrates superiority by outperforming other methods with high ADR and F1-score values. This is because of the ability of the KD metric to separate normal from abnormal pressure sensor data, which enables the KPCA-KD scheme to identify the deformity better than other schemes.

TABLE II
DETECTION RESULTS OF PCA, ICA AND KPCA FOR TWO ABNORMAL SCENARIOS

No.	Index	PCA			ICA				Kernel PCA		
		T^2	SPE	KD	I_d^2	I_e^2	SPE	KD	T^2	SPE	KD
1	ADR	93.74	4.26	14.93	36.09	45.86	69.19	96.85	97.74	99.75	100.00
	FAR	4.55	2.27	0.00	0.00	0.00	0.00	0.00	0.00	0.00	0.00
	Pre	95.41	66.00	100.00	100.00	100.00	100.00	100.00	100.00	100.00	100.00
	Rec	93.74	4.36	14.88	36.09	45.86	69.19	96.85	98.10	99.80	100.00
	F1-sc	94.29	8.00	25.98	53.15	62.80	81.78	98.39	98.85	99.87	100.00
2	ADR	5.26	95.24	96.74	34.42	39.78	43.48	70.83	8.77	51.58	99.25
	FAR	4.55	2.27	0.00	0.00	0.00	0.00	0.00	4.53	0.00	0.00
	Pre	53.00	97.69	100.00	100.00	100.00	100.00	100.00	66.00	100.00	100.00
	Rec	5.26	95.24	96.74	34.42	39.78	43.78	70.83	8.77	51.98	99.25
	F1-sc	10.72	96.46	98.35	51.21	56.91	60.60	82.92	15.07	68.05	99.62

b) Case 2:: The flat foot deformity identification of PCA and KPCA-based methods are depicted in Fig. 3 and Fig. 4, respectively. The results show that the T^2 based metrics are unable to identify this deformity and have poor detection rates, as seen in Table II. We also observe that the PCA-SPE and KPCA-SPE schemes can identify the abnormal condition better than PCA-T^2 and KPCA-T^2 schemes; there are few missed detections in these cases. The PCA-KD scheme performs better than the traditional PCA models, but it detects this abnormal condition with a small amount of delay that can be observed in the result plots. While ICA conventional indicators are unable to detect this abnormality with good ADR, the ICA-KD shows good detection performance. Compared to all other schemes, the KPCA-KD scheme can detect abnormal conditions with a high detection rate. Even from Table II, it may be observed that the KPCA-KD scheme outperforms other methods with good ADR and F1-score values.

Table III lists the aggregated performances per model. The proposed KPCA-KD scheme achieved the best detection performance with ADR = 99.63 and FAR=0. Results in Table III confirm that in terms of all metrics calculated, KPCA-KD is the best in detecting foot deformities with high efficiency and satisfying accuracy in the availability of small-sized data. It could be attributed to its capability to capture non-linearity using the KPCA model and the sensitivity of the KD-based detector in separating normal from abnormal data. However, it is worthwhile to notice that the three PCA-based methods (i.e., PCA-based T^2, SPE, and KD), as well as ICA-based methods (I_d^2, I_e^2, SPE and KD), exhibited limitations in this study by reaching slightly lower detection performance. This is because the PCA and ICA-based approaches perform a linear transformation on the plantar pressure measurements, and these data may not be linearly separable. Overall, this study highlights the potential of the KPCA-KD approach in detecting abnormal foot deformities in a small-sized plantar pressure dataset.

However, the proposed KPCA-KD approach cannot discriminate arched and flat foot deformities. To bypass this limitation, the support vector machine (SVM) method is applied only to the detected features to separate the two deformities. The SVM achieved an accuracy of 98.5%/, a true positive rate of 97%, and a false negative rate of 3%.

TABLE III
AVERAGED DETECTION PERFORMANCE FOR THE SIX INVESTIGATED MONITORING SCHEMES.

Approach	Precision	Recall	F1-score	ADR	FAR
PCA-T^2	0.74	0.50	0.53	49.50	4.55
PCA-SPE	0.82	0.50	0.52	49.75	2.27
PCA-KD	1	0.56	0.62	55.84	0
ICA-I_d^2	1	0.35	0.52	35.25	0
ICA-I_e^2	1	0.42	0.59	42.82	0
ICA-SPE	1	0.56	0.71	56.48	0
ICA-KD	1	0.83	0.91	83.84	0
KPCA-T^2	0.83	0.53	0.57	53.26	2.28
KPCA-SPE	1	0.76	0.84	75.67	0
KPCA-KD	1	1.00	1.00	99.63	0

Overall, a doctor can employ this approach as a decision support system to help diagnose individual patients for early diagnosis and physical rehabilitation. In addition, recording plantar pressure measurements of the patient in each session enables the assessment of patient evolution.

IV. CONCLUSION

Early detection of foot deformities (i.e., arched and flat feet), particularly in children, is crucial for early treatment and physical rehabilitation. This work introduces a semi-supervised data-driven technique to detect foot deformities based on plantar pressure measurements gathered using resistive pressure sensors. Besides detecting foot deformities, the approach does not require any labeled data. To this end, the modeling framework was provided by the KPCA approach, and the indicator of deformities was generated with the KD-based scheme. Specifically, the KD metric was computed between the residuals of training foot data and abnormal foot data. In addition, the threshold was computed using the non-parametric KDE approach to enable flexible detection. Results demonstrated the superiority of the KPCA-KD scheme in identifying the two-foot deformities in comparison to PCA-T^2, PCA-SPE, PCA-KD, ICA-I_d^2, ICA-I_e^2, ICA-SPE, ICA-KD, KPCA-T^2 and KPCA-SPE based techniques respectively. The KPCA-KD scheme achieved the best detection performance with a lower FAR value, higher ADR, and high F1-score compared to other monitoring methods.

Although the proposed KPCA-KD monitoring strategy achieves improved monitoring performance, it cannot discriminate between flat and arched foot deformities. The SVM

classifier is applied here to identify flat from arched foot deformities. For future work, we plan to explore clustering methods to recognize the type of detected foot deformity in an unsupervised way. Also, in the absence of large-sized data, it would be interesting to generate augmented data via augmentation techniques to enable improving the construction of models and thus, enhance the task of detection.

REFERENCES

[1] M. N. Orlin and T. G. McPoil, "Plantar pressure assessment," *Physical therapy*, vol. 80, no. 4, pp. 399–409, 2000.
[2] A. H. Sabry, W. Z. W. Hasan, M. N. Mohtar, R. Ahmad, and H. R. Harun, "Plantar pressure repeatability data analysis for healthy adult based on EMED system," *Malaysian Journal of Fundamental and Applied Sciences*, vol. 14, no. 1, pp. 96–101, 2018.
[3] J. K. Gurney, U. G. Kersting, and D. Rosenbaum, "Between-day reliability of repeated plantar pressure distribution measurements in a normal population," *Gait & posture*, vol. 27, no. 4, pp. 706–709, 2008.
[4] G.-M. Jeong, P. H. Truong, and S.-I. Choi, "Classification of three types of walking activities regarding stairs using plantar pressure sensors," *IEEE Sensors Journal*, vol. 17, no. 9, pp. 2638–2639, 2017.
[5] P. D. Rosero-Montalvo, E. A. Fuentes-Hernández, M. E. Morocho-Cayamcela, L. M. Sierra-Martínez, and D. H. Peluffo-Ordóñez, "Addressing the data acquisition paradigm in the early detection of pediatric foot deformities," *Sensors*, vol. 21, no. 13, p. 4422, 2021.
[6] W. Li, W. Meng, and M. H. Au, "Enhancing collaborative intrusion detection via disagreement-based semi-supervised learning in iot environments," *Journal of Network and Computer Applications*, vol. 161, p. 102631, 2020.
[7] S. W. Choi, C. Lee, J.-M. Lee, J. H. Park, and I.-B. Lee, "Fault detection and identification of nonlinear processes based on kernel pca," *Chemometrics and intelligent laboratory systems*, vol. 75, no. 1, pp. 55–67, 2005.
[8] M. Nawaz, A. Shah Maulud, H. Zabri, H. Suleman, and L. Tufa Dendena, "Multiscale framework for real-time process monitoring of nonlinear chemical process systems," *Industrial and Engineering Chemistry Research*, vol. 59, pp. 18 595–18 606, 2020.
[9] J.-M. Lee, C. Yoo, S. W. Choi, P. A. Vanrolleghem, and I.-B. Lee, "Nonlinear process monitoring using kernel principal component analysis," *Chemical engineering science*, vol. 59, no. 1, pp. 223–234, 2004.
[10] K. R. Kini, M. Bapat, and M. Madakyaru, "Kantorovich distance based fault detection scheme for non-linear processes," *IEEE Access*, vol. 10, pp. 1051–1067, 2022.
[11] F. Harrou, Y. Sun, A. S. Hering, M. Madakyaru *et al.*, *Statistical process monitoring using advanced data-driven and deep learning approaches: theory and practical applications*. Elsevier, 2020.
[12] E. A. F.-H. P. D. R.-M. D. Peluffo, "Footstep analysis using pressure sensors," 2019. [Online]. Available: http://dx.doi.org/10.21227/kqm6-1877

K.Ramakrishna Kini (kr.kini@manipal.edu) received M.Tech. Degree in Control Systems and Ph.D. degree in advanced control system from Manipal Institute of Technology Manipal, Karnataka India. He is currently an Assistant Professor with Instrumentation and Control Engineering, Manipal Institute of Technology, Manipal Academy of Higher Education, India. His research interests are in data-driven fault detection and diagnosis, soft sensors, and machine learning methods.

Muddu Madakyaru (muddu.m@manipal.edu) received M.Tech. degree from NITK, India, a Ph.D. degree in process control from the IIT Bombay, Mumbai, India and Post-Doctoral Researcher with Texas AM University, Doha, Qatar. He is currently a Professor with the Department of Chemical Engineering, Manipal Institute of Technology, Manipal Academy of Higher Education, India. His research interests are in advanced process control, including system identification, fault detection and diagnosis, and machine learning methods.

Fouzi Harrou (fouzi.harrou@kaust.edu.sa) received an M.Sc. degree in telecommunications and networking from the University of Paris VI in 2006 and a Ph.D. degree in systems optimization and security in 2010 from the University Technology of Troyes (UTT), France. Dr. Harrou's research interests are in statistical anomaly detection and process monitoring with a particular emphasis on data-driven, machine learning/deep learning methods. He is IEEE senior member.

Ying Sun (ying.sun@kaust.edu.sa) is an Associate Professor of Statistics in the Division of Computer, Electrical and Mathematical Sciences and Engineering (CEMSE). She joined King Abdullah University of Science and Technology (KAUST) in June 2014 after one-year service as an Assistant Professor in the Department of Statistics at the Ohio State University, USA. At KAUST, she leads a multidisciplinary research group on environmental statistics, dedicated to developing statistical models and methods for space-time data to solve environmental problems.